IMPROVED LOW VOLTAGE RIDE-THROUGH SCHEME FOR PMSG-BASED WIND ENERGY CONVERSION SYSTEMS

Nguyen Minh Tien[1], Van Tan Luong[2,*], Nguyen Tan Thach[2]

[1]*Nha Trang College of Technology*

[2]*Ho Chi Minh City University of Industry and Trade*

*Email: *luongvt@huit.edu.vn*

Received: 6 December 2024; Accepted: 14 January 2025

ABSTRACT

This paper proposes a low-voltage ride-through (LVRT) scheme for the permanent magnet synchronous generator (PMSG) wind turbine system during the grid voltage sags. At the generator-side, the DC-link voltage controller is designed, based on particle swarm optimizaion (PSO). Meanwhile, at the line-side, the grid active power are regulated for a maximum power point tracking (MPPT) and the reactive power is controlled for the grid support through the reactive current control. The validity of this scheme has been verified by the simulation of the 2 MW-PMSG wind turbine system.

Keywords: Braking chopper, permanent magnet synchronous generator, low-voltage ride-through, wind turbine.

1. INTRODUCTION

Recently, the wind power generation has been considered as one of the fastest growing renewable energy sources in the world since the natural resources are gradually becoming exhausted. In the variable-speed wind turbine systems, compared with doubly-fed induction generator wind turbine system, a direct-drive wind energy conversion system using permanent magnet synchronous generator (PMSG) has more benefits such as no gearbox, high precision, high power density, and simple control method, except initial installation costs [1, 2].

Nowadays, wind energy power plants have extensively integrated into the utility grid [3] A low voltage ride through (LVRT) is considered as an essence for wind generators in the case of grid fault. Wind generators have to withstand voltage disturbances without being disconnected from the grid. As can be clearly seen from Figure 1, at the point of common coupling (PCC), the voltage be dropped up to 80% of the nominal value within 0.1 seconds after the fault clearance [3]. For a grid which is integrated with large size wind power plants, LVRT technique is an effective way to obtain the this objective.

Several solutions have been suggested for the LVRTs in the variable-speed wind turbine systems. For this purpose, a braking chopper consisting of a resistor of high power rating and a switch connected in parallel with DC-link of the PMSG to absorb the active power during the grid fault [4, 5]. The generator keeps working to generate the active power, while the LSC can control the grid reactive power or the voltage at the point of common coupling (PCC) according to the grid requirement. However, the LSC cannot provide enough reactive power or voltage support for the case of a weak grid, since the LSC is out of control. Also, a static synchronous compensator (STATCOM) is a device connected in the shunt to supply the reactive power to the system to regulate the voltage at PCC [6, 7]. Similarly, static VAR compensator (SVC) has been used to assist the improvement of steady state and transient performance for the system. The reactive power is injected by STATCOM to grid network during voltage sag can be higher than that supplied by the SVC. Also, energy storage system (ESS) consisting of a buck-boost converter, inductor and supercapacitor is connected in paralell with the DC-link capacitor for LVRT enhancement [8]. During the grid voltage fault, the ESS will absorb of the additional energy from DC-link to prevent its overvoltage. Although the STATCOM and ESS are a common solution for improving LVRT capabilities, using these added devices in a wind turbine system will raise the total cost of the system, in the case of the deep voltage.

Normally, DC-link voltage is controlled to reach its reference value at the line-side converter (LSC), while the generator -side converter (GSC) controls the real power feeding to the grid. When the grid voltage sags occur, the LSC in the aforementioned control method seems to be out of control. Since the wind turbine and generator still keep operating continuously, this leads to the excessive increase of the DC-link voltage. However, the generator power delivered to the grid is much reduced.

Several researches have focused on the DC-link voltage control schemes employed at the GSC instead of the LSC [9, 10]. By accelerating the generator speed during the grid voltage sag, the DC-link voltage can be controlled to keep constant value. On the one hand, the performance of the DC-link voltage is still not good when a proportional integral (PI) controller is used, depending on the relationship between the power and energy [9]. On the other hand, a nonlinear control technique has been applied to the DC-link voltage control for the PMSG wind turbine system [11]. Nevertheless, the dynamic response of the DC-link voltage is still high.

In the proposed method, the GSC controls the DC-link voltage based on particle swarm optimization, the LSC controls the real power for the MPPT, imaginary power for grid support, and braking chopper is applied to suppress the DC-link voltage during the grid voltage sags. The simulation using PSIM software for 2 MW-PMSG wind turbine system has been done to verify the effectiveness of the proposed method.

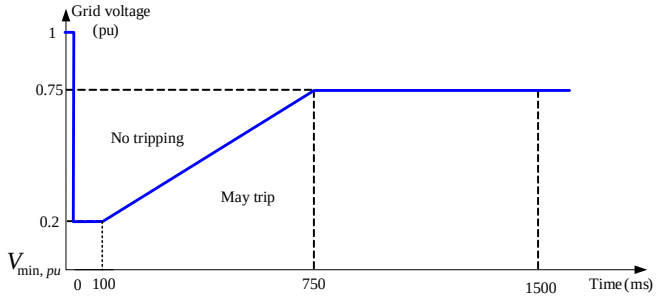

Figure 1. A grid code [3]

2. SYSTEM CONFIGURATION

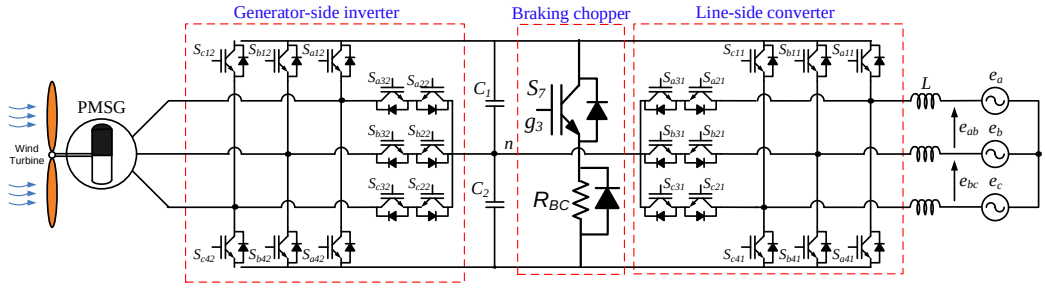

Figure 2. PMSG wind power system

Figure 2 shows the configuration of a direct-driven PMSG wind turbine system in which the generator is connected to the grid through the full-scale T-type three-level back-to-back PWM converters. The T-type converter is a simple extension of the two-level voltage source converter with an additional active bidirectional switch at the midpoint of DC-link. The T-type converter has the advantages of a low total harmonic distortion of the NPC converter as well as a simple operating principle of the two-level converter [12]. The modulation strategy for the three-level NPC converter is similar to the T-type converter. A braking chopper is connected in parallel with the DC-link. The BC will be activated to dissipate the excessive power in cases of deep voltage sags. In grid fault conditions, on the other hand, the functions of GSC and LSC are exchanged together so that the DC-link can not be directly affected by the grid.

3. MODELING OF WIND TURBINE SYSTEMS

3.1. Modeling of wind turbines

The output power of WT (P_t) is determined as [13]

$$P_t = \frac{1}{2}\rho\pi R^2 C_p\ \lambda,\beta\ V^3 \tag{1}$$

where ρ is the air density [kg/m^3], R is the radius of blade [m], V is the wind speed [m/s], and $C_p(\lambda, \beta)$ is the power conversion coefficient which is a function of the tip-speed ratio ($\lambda = \frac{R\omega_t}{V}$) and the pitch angle (β).

The turbine torque can be expressed as

$$T_t = \frac{1}{2}\rho\pi R^3 \frac{C_p\ \lambda,\beta}{\lambda} V^2 \tag{2}$$

3.2. Modeling of PMSG

The stator voltage equations of the PMSG are expressed in the synchronous d-q coordinates as [14]

$$\begin{bmatrix} V_{ds} \\ V_{qs} \end{bmatrix} = \begin{bmatrix} R_s + pL_s & -\omega_r L_s \\ \omega_r L_s & R_s + pL_s \end{bmatrix} \begin{bmatrix} I_{ds} \\ I_{qs} \end{bmatrix} + \begin{bmatrix} 0 \\ \omega_r \lambda_f \end{bmatrix} \tag{3}$$

where I_{ds} and I_{qs} are d, q-axis stator currents, R_s and L_s are stator resistance and inductance, respectively, λ_f is magnet flux, and ω_r is electrical angular speed.

For the generator with surface-mounted permanent magnets, d- and q-axis inductances are the same. Then, the electromagnetic torque T_e is expressed as

$$T_e = \frac{3}{2}\frac{p}{2}\lambda_f I_{qs} \tag{4}$$

where p is the number of poles.

The output electrical power can be calculated as

$$P_g = 1.5\left(V_{qs}I_{qs} + V_{ds}I_{ds}\right) \tag{5}$$

3.3. Modeling of shaft system

The turbine torque with one-mass modeling of wind turbine systems is expressed as [13]

$$J_t \frac{d\omega_t}{dt} = T_t - T_g \tag{6}$$

where J_t is the combined inertia of the turbine and generator and T_g is the generator torque.

4. PROPOSED CONTROL SCHEME

When the grid voltages are unbalanced, the operation of the LSC is directly affected. For this, the generator output power is limited when feeding to the grid. During this duration, the wind turbine and generator still keep working. Therefore, the generated power from the generator side may make the DC-link voltage increase. In this part, the DC-link voltage is controlled by the generator -side converter, while line-side converter controls maximum power point tracking (MPPT) and reactive power according to the grid through the reactive current control. To avoid the increase of the DC link voltage during the grid fault, a braking chopper has been used.

4.1. Control of generator -side converter

Particle Swarm Optimization (PSO) was first described in 1995 by James Kennedy and Russell C.Eberhart. They are a social psychologist and an electrical engineer. Several studies have demonstrated

the effectiveness of applying PSO into improving the control performance of reactive power, voltage and motor [15-17].

Unique to the concept of the PSO is flying potential solutions through hyperspace, accelerating toward "better" solutions. Each particle keeps track of its best solution (fitness) it has achieved so far. This value is called pbest. The best value tracked by any particle in the population is called gbest.The PSO concept consists of, at each time step, changing the velocity each particle toward its pbest and gbest locations.

The process of optimizing the PI parameters using PSO is performed as shown in Figure 3. This control method uses PI controller for the DC-link voltage of the back-to-back PWM converters. The purpose of applying the PSO algorithm is to search the optimal parameters for the PI controller to reduce the error between the output voltage of the LSC and its reference value. Thus, the fitness function for the system will be the error between the DC-link voltage and its reference voltage ($e(t)$) given by:

$$IAE = \int_0^{\infty} |e(t)| dt \tag{7}$$

In the simulation, the initial values are chosen as: c1 = 2; c2 = 2.2; w_{max} = 1.4; w_{min} = 0.1; the iteration is 1000.

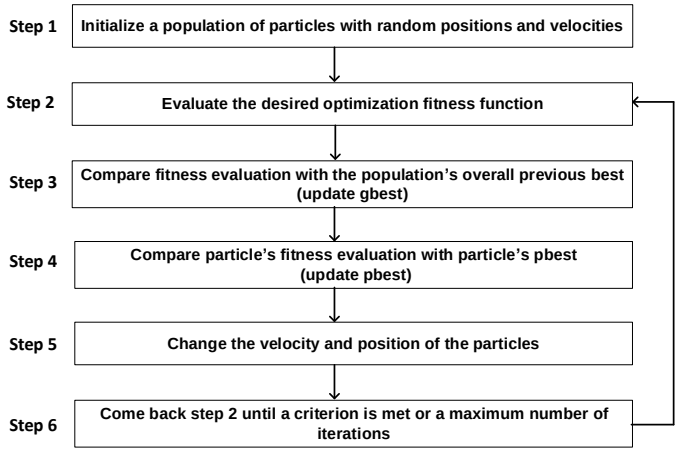

Figure 3. PSO algorithm for optimal PI controller

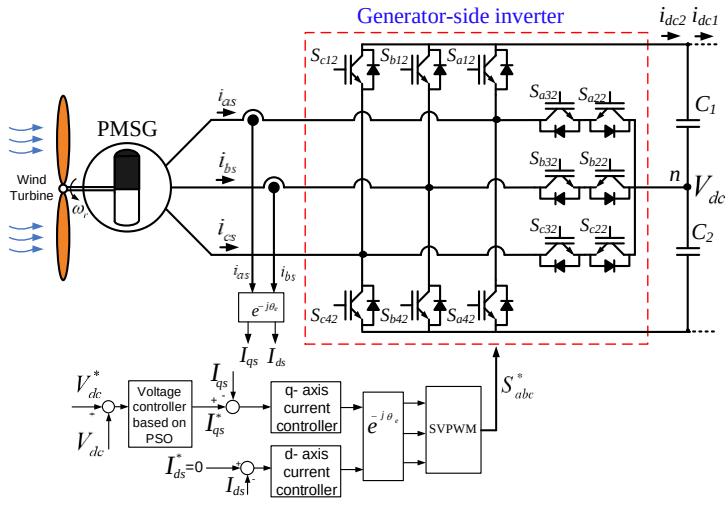

Figure 4. Control block diagram of the generator-side converter

The control block diagram of the GSC that includes the outer loop DC-link voltage PI controller based on PSO and the inner loop current controller for dq-axis components is shown in Figure 4.

4.2. Control of line-side converter

4.2.1. Grid power reference

The dynamic characteristics of wind turbine system using PMSG are expressed as

$$P_g = P_t - J_t\omega_t \frac{d\omega_t}{dt} \tag{8}$$

$$P_{cap} = CV_{dc}\frac{dV_{dc}}{dt} = P_g - P_{grid} \tag{9}$$

where P_g is the generated power, P_{grid} is the grid power, P_{cap} is the DC-link capacitor power, V_{dc} is the DC-link voltage, C is the DC-link capacitor.

From (8) and (9), the grid power reference is given from V_{dc} and ω_t as

$$P_{grid}^{*} = K_{opt}\cdot\omega_t^3 - J_t\frac{\omega_t d\omega_t}{dt} - C\frac{V_{dc}dV_{dc}}{dt} \tag{10}$$

Where K_{opt} is optimal power coeficient.

4.2.2. Grid current references

Under unbalanced grid voltage conditions, the components of the DC power (P_0 , Q_0) and second-order components of power (P_{c2} , P_{s2} , Q_{c2} , Q_{s2}) caused by the positive and negative sequence components of grid voltages (E_d^+ , E_q^+ , E_d^- , E_q^-) and currents (I_d^+ , I_q^+ , I_d^- , I_q^-) due to grid fault are represented in a matrix form as [18]

$$\begin{bmatrix} P_0 \\ Q_0 \\ P_{s2} \\ P_{c2} \end{bmatrix} = 1.5D \begin{bmatrix} I_d^+ \\ I_q^+ \\ I_d^- \\ I_q^- \end{bmatrix} \tag{11}$$

Where $D = \begin{bmatrix} E_d^+ & E_q^+ & E_d^- & E_q^- \\ E_q^+ & -E_d^+ & E_q^- & -E_d^- \\ E_q^- & -E_d^- & -E_q^+ & E_d^+ \\ E_d^- & E_q^- & E_d^+ & E_q^+ \end{bmatrix}$

From (11), the positive- and negative-sequence components of the grid current references are expressed as

$$\begin{bmatrix} I_d^{+*} \\ I_q^{+*} \\ I_d^{-*} \\ I_q^{-*} \end{bmatrix} = \frac{2}{3}D^{-1} \begin{bmatrix} P_{grid}^{*} \\ Q_{grid}^{*} \\ 0 \\ 0 \end{bmatrix} \tag{12}$$

Where $Q_{grid}^{*} = \left(2.186 - 2.571\frac{E_{grid}}{E_{grid.\max}}\right)\cdot 2Q_{\max}$ must be subject to $S_{rated} = \sqrt{P_{grid}^{*2} + Q_{grid}^{*2}}$ [3]

The current controllers for positive-sequence components and negative-sequence components using PI controller are shown in Figure 5.

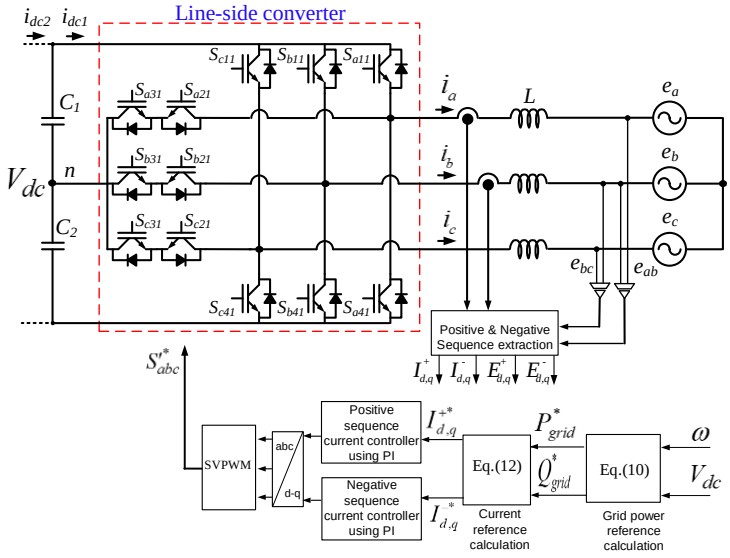

Figure 5. Control block diagram of the line-side converter

4.3. Braking chopper control

A braking chopper circuit consisting of a resistor and a switch is connected in paralell with the DC-link capacitor to reduce the overvoltage as well as voltage-fluctuation of the DC-link in the case of grid voltage sags. Neglecting the power losses of the converters, since the extra energy is dissipated by the resistor of the braking chopper and thus, the DC-link voltage fluctuation can be suppressed, the duty ratio D_1 for the switch depending on $\left(P_{LSC} - P_{GSC}\right)$ is obtained as

$$D_3 = \frac{R_{BC}}{V_{dc}^2}\left(P_{LSC} - P_{GSC}\right) \tag{13}$$

where R_{BC} is the braking resistance, P_{LSC} and P_{GSC} are the grid power and generator power, respectively.

5. SIMULATION AND RESULTS

The simulation using the PSIM software for a 2-MW PMSG wind turbine has been performed to verify the validity of the proposed method. The parameters of the wind turbine and PMSG are listed in Table 1 and 2, respectively. The reference value of the DC-link voltage is 1.3 kV, the DC-link capacitor is 0.1 F, the switching frequency is 2 kHz, and the grid voltage is 690 V_{rms}/60 Hz.

Table 1. Parameters of wind turbine

Parameters	Values
Rated power	2 MW
Blade radius	45 m
Air density	1.225 kg/m^3
Max. power conv. coefficient	0.411
Cut-in speed	3 m/s
Cut-out speed	25 m/s
Rated wind speed	16.1 m/s
Blade inertia	6.3x10^6 kg.m^2

Table 2. Parameters of PMSG

Parameters	Values
Rated power	2 MW
Grid voltage	690 V
Stator voltage/frequency	690 V/60 Hz
Stator resistance	0.008556 Ω
d-axis inductance	0.00359 H
q-axis inductance	0.00359 H

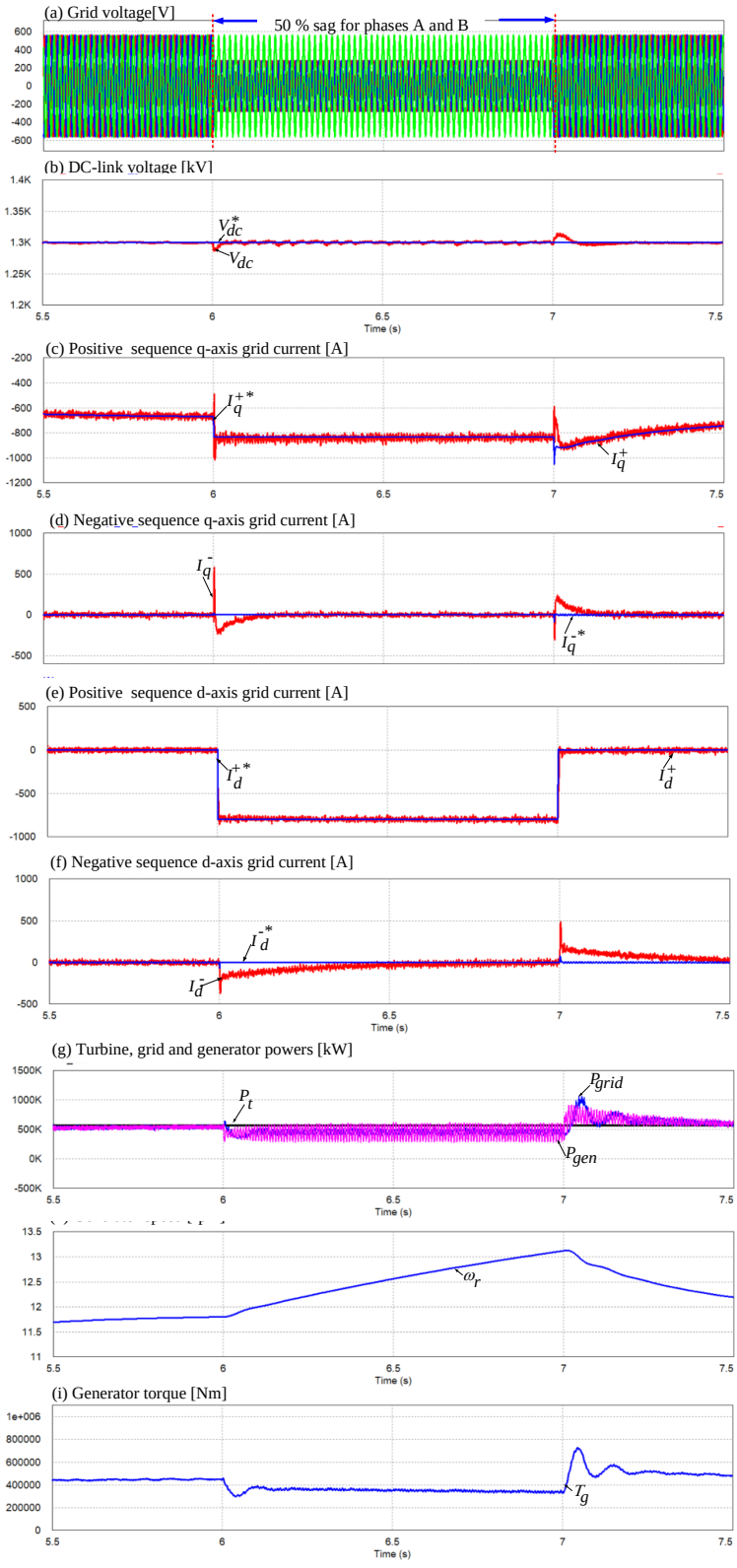

Figure 6. Wind turbine system performance for three-phase unbalanced voltage sag (50% sag for phases A and B). (a) Grid voltage. (b). DC-link voltage. (c) Positive sequence q-axis grid current. (d) Negative sequence q-axis grid current.(e) Positive sequence d-axis grid current. (f) Negative sequence d-axis grid current. (g) Turbine, grid and generator powers. (h) Generator speed. (i) Generator torque.

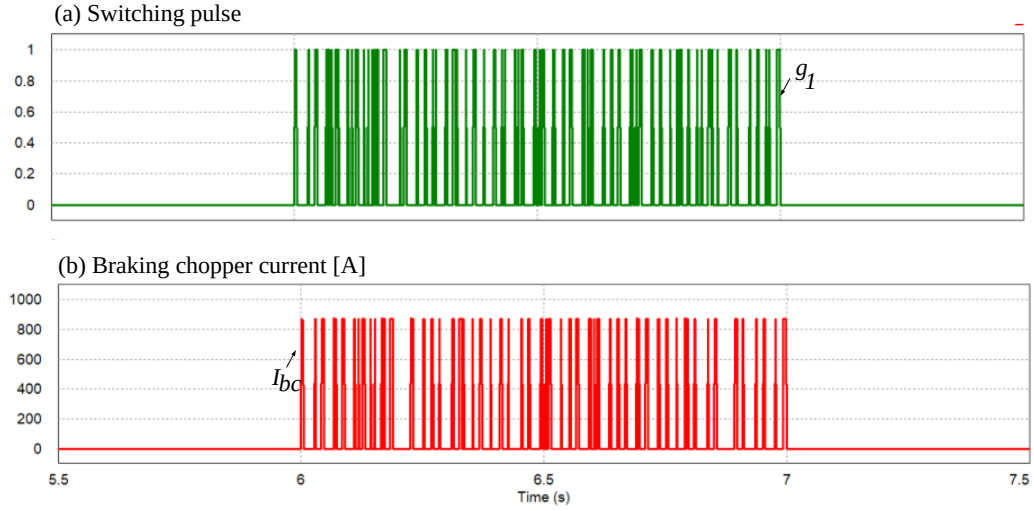

Figure 7. Response of BC under unbalanced sags. (a) Switching pulse. (b) Braking chopper current.

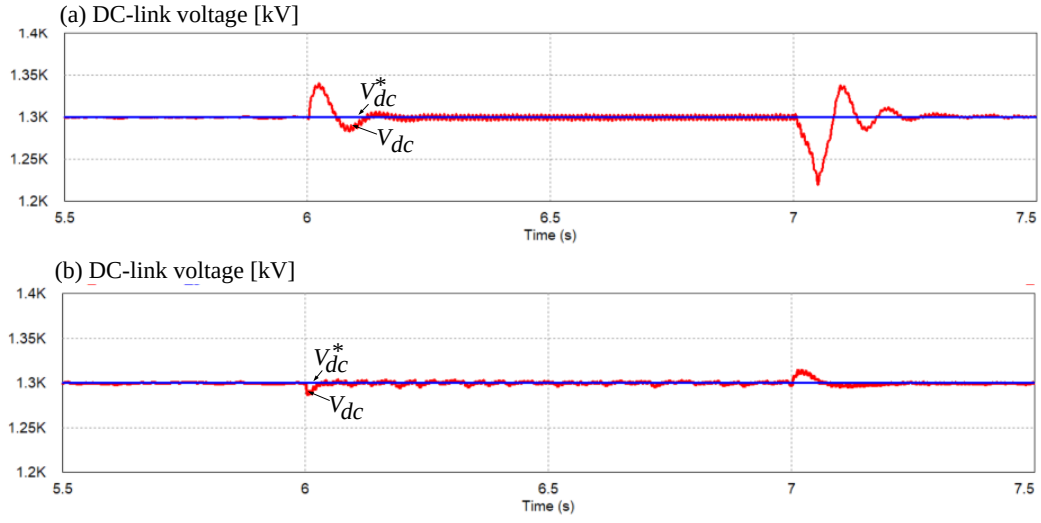

Figure 8. Comparison of DC-link voltage responses under unbalanced sag using:
(a) conventional PI controller. (b) proposed method.

Figure 6 shows the system performance for a grid unbalanced voltage sag, in which the wind speed is set to be 7 m/s for easy investigation. The fault condition is 50% sag for phases A and B, for 1 sec (60 cycles), as shown in Figure 6 (a). Figure 6(b) shows the response of DC-link voltage. Also, the grid currents in positive and negative sequence q-axis are illustrated in Figure 6(c) and 6(d). Moreover, the grid currents in positive and negative sequence d-axis are given in Figure 6(e) and 6(f), in which the reference value of the grid currents in positive sequence d-axis is calculated in (12). Since the grid voltage sag is unbalanced, the positive-sequence q-axis voltage is decreased and the negative-sequence voltage components in dq axis occur, the grid and generator powers are reduced, as illustrated in Figure 6(g). During the grid fault duration, the wind turbine must accelerate to deliver the generated power to the grid. Thus, the generator speed is increased to keep the DC-link voltage constant, as shown in Figure 6(b). Similarly to power, the generator torque is also reduced during the period time of grid fault.

Figure 7 shows the responses of the braking chopper in the case of unbalanced sag. Since the difference between the generator and line powers can not deliver to the grid fully, the rest of the power is dissipated by the braking chopper, when the switch is on. The switching pulse for this switch is shown in Figure 7 (a) and the current flowing the resistor of the braking chopper is given in Figure 7 (b).

Figure 8 shows the DC-link voltage responses in the cases of the conventional PI control and

proposed control methods. The proposed method gives faster transient response and lower overshoot. The values of percentage of overshoot for the DC-link voltage using the conventional PI control and proposed control methods are 3.077% and 0.769%, respectively in comparison with its reference.

6. CONCLUSION

This paper presents the LVRT scheme for the permanent magnet synchronous generator wind turbine system. At the grid fault, a PI controller based on PSO is applied for the DC-link voltage control at the generator-side converter, while the MPPT control and the reactive current control for the grid support are done at the line-side converter. Also, BC is used to enhance a LVRT capability for the wind turbines when the grid voltage is dropped. The validity of the proposed control has been verified by simulation results for 2 MW PMSG wind power system.

REFERENCES

1. Chinchilla, M., S. Arnaltes and J. C. Burgos. - Control of permanent-magnet generators applied to variable-speed wind-energy systems connected to the grid. IEEE Transactions on Energy Conversion **21** (1) (2006) 130-135. https://doi.org/10.1109/TEC.2005.853735
2. Polinder, H. , F. F. A Van Der Pijl and P. Tavner. - Comparison of direct-drive and geared generator concepts for wind turbines. IEEE Transactions on Energy Conversion **21** (3) (2006) 543-550. https://doi.org/10.1109/TEC.2006.875476
3. Iov F., Hansen A.D., Sørensen P., and Cutululis N. A. - Mapping of grid faults and grid codes, Technical Report Risø-R-1617(EN), Risø National Laboratory, Technical University of Denmark, Roskilde, Denmark (2007).
4. Howlader A. M. and Senjyu T. - A comprehensive review of low voltage ride through capability strategies for the wind energy conversion systems, Renew. Sustain. Energy Rev., **56** (2016) 643–658. https://doi.org/10.1016/j.rser.2015.11.073
5. Hansen A. D. and Michalke G. - Multi-pole permanent magnet synchronous generator wind turbines' grid support capability in uninterrupted operation during grid faults, IET Renewable Power Generation **3** (3) (2009) 333-348. https://doi.org/10.1049/iet-rpg.2008.0055
6. Chen Z., Guerrero J. M., and Blaabjerg F., -A review of the state of the art of power electronics for wind turbines, IEEE Transactions on Power Electronics **24 (**8) (2009) 1859–1875. https://doi.org/10.1109/TPEL.2009.2017082
7. Molinas M., Suul J. A., and Undeland T. -Low voltage ride through of wind farms with cage generators: STATCOM Versus SVC, IEEE Transactions on Power Electronics **23** (3) (2008) 1104–1117. https://doi.org/10.1109/TPEL.2008.921169
8. Nguyen T. H. and Lee D.-C. -Ride-through technique for PMSG wind turbines using energy storage systems, Journal of Power Electronics **10 (**6) (2010) 733–738.
9. Yuan X. , Wang F., Boroyevich D., Li Y. and Burgos R. - DC-link voltage control of a full power converter for wind generator operating in weak-grid systems. IEEE Transactions on Power Electronics **24** (9) (2009) 2178-2192. https://doi.org/10.1109/TPEL.2009.2022082
10. Davari M. and Mohamed Y. A.-R. I. - Robust DC-Link Voltage Control of a Full-Scale PMSG Wind Turbine for Effective Integration in DC Grids, IEEE Transactions on Power Electronics **32** (5) (2017) 4021–4035. https://doi.org/10.1109/TPEL.2016.2586119
11. Kim K. H., Jeung Y. C., Lee D. C., and Kim H. G., -LVRT scheme of PMSG wind power systems based on feedback linearization, IEEE Transactions on Power Electronics **27** (5) (2012) 2376-2384. https://doi.org/10.1109/TPEL.2011.2171999
12. Schweizer M. and Kolar J. W. -Design and implementation of a highly efficient three-level t-type converter for low-voltage applications, IEEE Transactions on Power Electronics **28 (**2) (2013) 899-907. https://doi.org/10.1109/TPEL.2012.2203151

13. Akhmatov V. - Induction generators for wind power, Multi-Science Publishing Company, (2005).
14. Nguyen T. H., Jang S.-H., Park H.-G. and Lee D.-C.- Sensorless control of PM synchronous generators for micro wind turbines. Proc. of IEEE PECON, Dec. 2008, pp. 936-941. https://doi.org/10.1109/PECON.2008.4762607
15. Liu C.H., Hsu Y.Y. - Design of a Self-Tuning PI Controller for a STATCOM Usin g Particle Swarm Optimization, IEEE Transactions on Industrial Electronics **57** (2) (2010) 702-715. https://doi.org/10.1109/TIE.2009.2028350
16. Gaing Z.-L. - A particle swarm optimization approach for optimum design of PID controller in AVR system, IEEE Transactions on Energy Conversion **19** (2) (2004) 384–391. https://doi.org/ 10.1109/TEC.2003.821821
17. Mahmud Iwan Solihin, Lee Fook Tack and Moey Leap Kean - Tuning of PID controller using particle swarm optimization (PSO), Proceeding of the International Conference on Advanced Science, Engineering and Information Technology (2011) 458-461. https://doi.org/ 10.18517/IJASEIT.1.4.93
18. Song H.-S. and Nam K.- Dual current control scheme for PWM converter under unbalanced input voltage conditions. IEEE Transactions on Industry Application **46** (5) (1999) 953-959. https://doi.org/ 10.1109/41.793344

TÓM TẮT

CHIẾN LƯỢC ĐIỀU KHIỂN LƯỚT QUA ĐIỆN ÁP THẤP NÂNG CAO CHO HỆ THỐNG CHUYỂN ĐỔI NĂNG LƯỢNG GIÓ DÙNG MÁY PHÁT PMSG

Nguyễn Minh Tiến[1], Văn Tấn Lượng[2,*], Nguyễn Tân Thạch[2]
[1]*Trường Cao đẳng Kỹ thuật Công nghệ Nha Trang*
[2]*Trường Đại học Công thương Thành phố Hồ Chí Minh*
*Email: *luongvt@huit.edu.vn*

Bài báo này đề xuất một chiến lược lướt qua điện áp thấp (LVRT) cho hệ thống tua bin gió dùng máy phát điện đồng bộ nam châm vĩnh cửu (PMSG) khi lưới có sụt áp lưới. Ở phía máy phát, bộ điều khiển điện áp DC-link được thiết kế dựa trên tối ưu hóa bầy đàn hạt (PSO). Trong khi đó, ở phía lưới, công suất tác dụng được điều chỉnh để dò tìm điểm phát công suất cực đại (MPPT) và công suất phản kháng được điều khiển để hỗ trợ lưới thông qua điều khiển dòng điện phản kháng. Tính khả thi của chiến lượt này đã được kiểm chứng thông qua việc mô phỏng hệ thống tua bin gió 2 MW-PMSG

Từ khóa: Braking chopper, máy phát điện đồng bộ nam châm vĩnh cửu, lướt qua điện áp thấp, tua bin gió.